Monitoring particulate material formation in a kraft furnace recovery boiler

Andréa O. S. Costa, Maurício B. de Souza Jr., Evaristo C. Biscaia Jr., and Enrique L. Lima

ABSTRACT: This study considers the potential use of neural networks to monitor particulate material formation during recovery boiler furnace operation. We built neural networks using 12 months of normal industrial operation data. The networks inputs were chosen according to available industrial information and process knowledge. The networks output describes the number of particles produced per minute. We initially used feed-forward neural networks, but the results were unacceptable because the information from normal operation data was inadequate. As an alternative approach, we investigated using discrete radial basis function networks to classify the amount of particles in size intervals. The results show that the proposed methodology can satisfactorily describe the particulate material formation, mainly as a monitoring tool for plant operation.

Application: This work advances efforts to enhance recovery boiler operations and control.

Many physical and chemical transformations occur during the burning of black liquor in furnace recovery boilers (**Fig. 1**). The process is usually described in distinct stages that can occur sequentially (1-9):

- *Drying stage*: black liquor particle loses its residual humidity;
- *Pyrolysis stage*: the particle increases its volume because of the generation of combustion gases, mainly total reduced sulphur (TRS: CH_3SH, CH_3SCH_3, $CH_3S_2CH_3$), SO_2, CO_2, CO, CH_4, and H_2O;
- *Char burning stage*: the particle volume reduces, which increases its density;
- *Oxidation and reduction of the inorganic salts stages*: the inorganic salts melt in the furnace bottom (char bed region), forming a fluid rich in Na_2S (called "smelt"), that flows out of the boiler.

In addition to the phenomena described above, particulate material (or simple particulate) is also formed during black liquor combustion. This material, composed of unburned liquor particles and inorganic salts (chemistry dust), is carried out, forming deposits on the tube surface in the upper boiler (10-12). Massive material accumulation will decrease the heat transfer efficiency of the recovery boiler, resulting in a lower superheated steam production. These deposits also can cause tube corrosion or plugging, requiring an unplanned shutdown of the equipment (10, 13) and, therefore, frequently limiting the system operation period. To remove the particulate in the combustion air, recovery boilers are equipped with sootblowers and electrostatic precipitators that operate with efficiencies above 99% (14).

The major components of the chemistry dust are Na_2SO_4 and Na_2CO_3 (13). According to Jokiniemi *et al.* (15) and Lefebvre and Santyr (16), the particulate formation occurs predominantly during the drying stage, the char burning stage, and as a result of the chemical reactions between the combustion air and substances coming from the smelt. Jokiniemi *et al.* (15) state that the particulate formation mechanism is not completely known. Janka *et al.* (17) consider that the particulate formation depends on the structural and operational characteristics of the recovery boiler and on the black liquor elementary chemical composition.

Advances in sootblower design and improved air delivery systems have helped to decrease problems associated with incrustation in the recovery boiler (13). However, as boilers are frequently pushed to higher liquor loads, there is more particulate formation leading to more deposit formation, making incrustation formation a challenge for all recovery boilers (13). In this context, we propose a methodology to model the particulate formation in the furnace recovery boiler, aiming at an indirect measurement of the incrustation potential for each adopted operational condition.

METHODOLOGY

As the particulate formation mechanism is not completely known, we chose an empirical methodology to model this phenomenon in an industrial recovery boiler. To this end, during a period of 12 months, we collected and treated industrial data to reduce the experimental errors. We used 3381 data sets for the network training and validation procedures. Using industry supplied information and the analysis of the industrial database, Costa *et al.* (18) have listed the major operational variables that affect the particulate formation (**Table I**). These variables are shown in **Figs. 2** and **3**. The output *Epart* describes the number of particles per minute (npp) passing through a specific region of the furnace. **Figure 4** shows that the used data sets are not evenly distributed along the studied operation region (Epart values are mainly located below 200 npp).

Variables	
Vvlu	black liquor feed
x	black liquor solid concentration
Tlu	black liquor feed temperature
Var1	primary air feed
Var2	secondary air feed
Var3	tertiary air feed
Par1	primary air feed pressure
Par2	secondary air feed pressure
Tar1	primary air feed temperature
Tar2	secondary air feed temperature
PI	black liquor feed pressure
Epart	number of particles per minute produced in the furnace

I. Operational variables (18).

Initial tests showed that linear models are inadequate to describe the particulate formation (see the low correlations values in **Table II**). We then tested feedforward neural networks and radial basis function (RBF) networks to model the process.

Operational variables	*Correlation values between the operational variables and Epart*
Vvlu	-0.1683
x	0.0568
Tlu	-0.1847
Var1	0.1777
Var2	-0.1601
Var3	-0.2840
Par1	-0.0820
Par2	-0.2930
Tar1	0.1073
Tar2	-0.0201
PI	0.2223

II. Correlation values between the major operational variables and Epart.

RESULTS

We first investigated different structures of the popular three-layers feedforward neural networks, considering linear activation function for the input layer and tan-sigmoid activation functions for the hidden and output layers. We trained the system over 1000 epochs using a backpropagation algorithm and 2705 data sets.

The evaluation of each neural network's prediction efficiency was accomplished using the sum of the squared errors of validation and training stages, and also graphical methods. The best feedforward neural network obtained has nine inputs (Vvlu, Tlu, Var1, Var2, Var3, Par1, Par2, Tar2, PI) and 12 neurons in the hidden layer. **Figures 5-8** depict results for the training and validation stages.

The prediction efficiency of the best feedforward neural network is not uniform. The neural network presents reduced prediction efficiencies, especially for Epart values larger than 300 npp, as a consequence of the small amount of training data for these Epart values (Fig. 4). Thus, we decided to investigate an approach using RBF neural networks to classify particulate material emission in discrete size intervals.

Two-thirds of the data, randomly chosen, were used in the training stage of the RBF networks. The remaining data were used during the networks validation tests. A maximum of 60 nodes was adopted for the hidden layer and, excluding the Epart variable, the other 11 operational variables listed in Table I were considered as probable inputs to the RBF networks.

During the training stage of each RBF network, we rejected variables considered not significant to the model accuracy. For this, a sensitivity analysis was accomplished on the neural network inputs (19). To define the sensitivity of a particular variable, test data were used to run the RBF network. After this, the accumulated prediction error was calculated for all the inputs. In the next step, the same data set and a constant value for the studied input (medium value) were used to obtain a new accumulated prediction error. We compared these errors and evaluated the importance of the applied modification in the empiric model. This procedure was repeated for each input. Thus, the variables that had less significance for the model accuracy or increased the prediction error were rejected.

Seven different classes were initially considered for Epart, each class representing a specific range of the variable (**Fig. 9**). Several RBF networks were proposed; the three best models obtained are presented in **Table III**.

	Network 1	Network 2	Network 3
Number of hidden nodes	23	29	31
Number of inputs	10	10	10
Input variables (in order of importance	Var2, Par2, Var1, Tar1, Par1,Tar2, x, PI, Var3, Tlu	Par2, Var2, Var1, Par1, Tar1, Tar2, x, Var3, PI, Tlu	Par2, Var2, Var1, Tar1, Tar2, Par1, Var3, PI, Tlu, Vvlu
Correct classification (%) (training/validation)	54.4/56.7	55.0/58.0	54.7/58.8
Class	Correct classification (%) considering all data		
1	0	0	0
2	92.5	93.4	90.9
3	32.8	34.6	37.3
4	0	0	0
5	0	0	0
6	0	0	0
7	0	0	0

III: Performance and characteristics of the three better networks obtained for an output distribution in seven classes (Fig. 9).

When the particulate formation was classified in seven classes, the best RBF networks obtained correctly classified about 54% of the training data and 58% of the validation data (Table II). However, considering each class individually, results showed good prediction capacity for class 2 (above 90%), followed by class 3 with a prediction efficiency of only about 35%. As these two classes represent more than 70% of the data, the RBF network training was probably excessively influenced by this fact, causing poor prediction efficiencies for the other classes (Table III). Therefore, aiming at an increase of the influence of more data ranges on the training stage, we combined classes 5, 6, and 7 to form a new distribution (**Fig. 10**).

The results presented in **Table IV** show that, considering the training data, the validation data, or each class separately, the three best networks obtained for the new distribution (Fig. 4) have prediction efficiencies slightly better than the previous ones (Table III). However, the prediction efficiencies still are not satisfactory, so we again adopted the strategy of combining classes. Three new distributions were proposed (**Figs. 11** [four classes], **12** [three classes] and **13** [two classes]). The best RBF networks obtained for each new distribution are presented in **Tables V-VII**, respectively.

	Network 1	Network 2	Network 3
Number of hidden nodes	30	45	46
Number of iputs	10	10	10
Input variables (in order of importance)	Par2, Var2, Var1, Tar1, Par1,Tar2, PI, Var3, x, Tlu	Par2, Var2, Var1, Tar2, Par1, Tar1, x, Var3, Tlu, PI	Par2, Var2, Var1, Par1, Tar2, Tar1, x, Var3, PI, Tlu
Correct classification (%) (training/validation)	56.0/57.1	56.2/57.3	55.6/59.2
Class	Correct classification (%) considering all data		
1	0.0	1.0	0.0
2	91.5	92.1	91.9
3	36.2	32.7	33.2
4	0.0	0.0	3.8
5	22.3	29.4	32.0

IV: Performance and characteristics of the three better networks obtained for an output distribution in five classes (Fig. 10).

	Network 1	Network 2	Network 3
Number of hidden nodes	17	23	40
Number of iputs	10	10	10
Input variables (in order of importance)	Var1, Par2, Var2, Par1, Tar1, Tar2, x, PI, Var3, Tlu	Par2, Var2, Var1, Par1, Tar1, Tar2, x, Var3, PI, Tlu	Par2, Var1, Var2, Tar2, Par1, Tar1, Var3, x, PI, Tlu
Correct classification (%) (training/validation)	58.2/57.1	57.6/57.6	58.2/58.7
Class	Correct classification (%) considering all data		
1	0.0	0.2	1.2
2	92.1	91.5	91.2
3	19.2	23.1	31.0
4	45.1	45.7	33.8

V. Performance and characteristics of the three better networks obtained for an output distribution in four classes (Fig. 11).

	Network 1	network 2	network 3
Number of hidden nodes	15	18	19
Number of inputs	10	10	10
Input variables (in order of importance)	Par2, Var2, Var1, Par1, Tar1, PI, x, Tar2, Tlu, Var3	Par2, Var2, Var1, Tar1, Par1, Tar2, PI, x, Tlu, Var3	Par2, Var2, Var1, Par1, Tar1, PI, Tar2, x, Tlu, Var3
Correct classification (%) (training/validation)	73.4/74.7	73.2/74.9	73.4/76.1
Class	Correct classification (%) considering all data		
1	94.0	92.7	93.7
2	41.7	44.3	42.6
3	0.0	0.0	7.1

VI. Performance and characteristics of the three better networks obtained for an output distribution in three classes (Fig. 12).

	Network 1	network 2	network 3
Number of hidden nodes	32	32	32
Number of inputs	4	5	9
Input variables (in order of importance)	Var1, Par2, Par1, Tlu	Par2, Var1, Par1, Var3, Tlu	Par2, Var1, Var2, Par1, Tar1, Tar2, Var3, Tlu, Vvlu
Correct classification (%) (training/validation)	79.7/78.3	80.8/80.1	79.5/80.0
Class	Correct classification (%) considering all data		
1	79.2	80.6	79.7
2	79.2	80.2	79.7

VII. Performance and characteristics of the three better networks obtained for an output distribution in two classes (Fig. 13).

By decreasing the number of classes considered for Epart, we obtained more accurate models to describe the number of particles formed in the furnace. As expected, for all distributions, the networks present better prediction efficiencies for the classes that have the largest number of data. However, the models are expected to be able to predict the particulate formation mainly when this phenomenon occurs in a large scale (implying large values of Epart). As this situation is avoided during normal operation, industrial data rarely describe operation conditions with large values of Epart. Consequently, networks with satisfactory prediction efficiency were obtained only when two classes were considered for Epart (Fig. 13, Table VII).

The results in Table VII show that the best three networks have a reduced number of inputs (4, 5, and 9), different from the other distributions, where 10 operational variables were necessary to describe the number of formed particles. Results for all studied distributions (Tables III-VII) showed that the most important variables considered to describe the process are related to the primary and secondary air feeds. This result agrees with industry observations that these variables are the ones that affect the process most.

We ran additional tests, repeating the operational data that have Epart values above 200 npp, to see if we could obtain more accurate models, resulting in a larger data base used to train new RBF networks.

However, the obtained networks did not present better prediction efficiency when compared to the networks previously calculated and the strategy was abandoned.

CONCLUSIONS

In this work, we used industrial data to build an empirical model that describes particulate formation in the kraft furnace recovery boiler. We observed that, because of an irregular distribution of the available data, it was not possible to obtain an acceptable feedforward neural network model completely describing the number of particles formed as a function of the operational conditions of the system.

This problem was solved using a different approach for the neural network output that, instead of considering all the possible numbers of particle formed, considers just a few particle number intervals. It should be noted that these kind of information is normally sufficient for a good furnace operation.

Therefore, discrete RBF networks were used to model the particulate formation. The best model has prediction efficiency around 80%, obtained when only two ranges of particles number were considered for the output variable (Epart). This small number of ranges is a consequence of the use of data provided by industry, where the reduction of particulate is an objective. Certainly, more precise and more detailed empirical models could be obtained using the proposed strategy if the operational data were distributed more evenly in a large number of particles ranges, but this requires an experimental planning procedure of difficult implementation in an industrial plant. Notwithstanding, it should be noted that the simple model obtained in this work represents a useful tool for particle production monitoring during the black liquor burning process, as it gives the operator and indication of abnormal operations.

Besides, the obtained results indicate that the particulate formation in the studied recovery boiler furnace has been affected decisively by the primary and secondary air feeds, a fact previously observed by the plant operator. This result should not be extrapolated to other recovery boilers since it is based on an empirical study, but the proposed approach can certainly be used after collecting the corresponding data. **TJ**

ACKNOWLEDGEMENTS

We acknowledge the financial support provided by CNPq–Conselho Nacional de Desenvolvimento Científico e Tecnológico, and technical support from Klabin Paraná Papéis.

LITERATURE CITED

1. Grace, T.M., in *Proceeding of the International Chemical Recovery Conference*, PAPTAC-TAPPI, Whistler, (2001), pp. 215-220.
2. Adams, T.N. in *Kraft Recovery Boilers* (T.N. Adams, Ed.), TAPPI PRESS, Atlanta, Georgia, USA, 1997, pp. 3-38.
3. Frederick, W.J., Hupa M., and Uusikartano T. *Bioresource Tech.* 48: 59(1994). *Cited by:* Sricharoenchaikul, V., Hicks, A.L., and Frederick, W.J. *Bioresource Tech.* 77: 131(2001).
4. Sricharoenchaikul, V., Hicks, A.L., Frederick, W.J. *Bioresource Tech.* 2001 77: 131(2001).
5. Macek, A., *Process Energy Combustion Sci.* 25: 275(1999).
6. Adams, T.N. in *Kraft Recovery Boilers* (T.N. Adams, Ed.), TAPPI PRESS, Atlanta, Georgia, USA, 1997, pp. 3-38.
7. Grace, T.M., in *Chemical Recovery in the Alkaline Pulping Processes* (R.P. Green and G. Hough, Eds.), TAPPI PRESS, Atlanta, (1992), pp. 57-78.
8. Frederick, W.J. and Hupa, M. in *Kraft Recovery Boilers* (T.N. Adams, Ed.), TAPPI PRESS, Atlanta, Georgia, USA, 1997, pp. 131-160.
9. Frederick, W.J. and Hupa, M. in *Kraft Recovery Boilers* (T.N. Adams, Ed.), TAPPI PRESS, Atlanta, Georgia, USA, 1997, pp. 131-160.
10. Mikkanen, P., Jokiniemi, J.K., Kauppinen, E.I. and Vakkilainen, E.K. *Fuel* 80(7): 987(2001).
11. Baxtel, L. L., Lind, T., Rumminger, M. and Kauppinene, E., T. M., in *Proceeding of the International Chemical Recovery Conference*, PAPTAC-TAPPI, Whistler, (2001), pp. 65-69.
12. Ansari, A. S. and Pandis, S. N. *Atmospheric Environment*, 33(5): 745(1999).
13. Tran, H. in *Kraft Recovery Boilers* (T.N. Adams, Ed.), TAPPI PRESS, Atlanta, Georgia, USA, 1997, pp. 247-282.

14. Lisa, K. in *Kraft Recovery Boilers* (T.N. Adams, Ed.), TAPPI PRESS, Atlanta, Georgia, USA, 1997, pp. 215-244.
15. Jokiniemi, J.K., Pyykönen, J., Mikkanen, P., and Kauppinen, E.I. *TAPPI J.* 79(7): 171(1996).
16. Lefebvre, B. and Santyr, G. in *Chemical Recovery in the Alkaline Pulping Processes* (R.P. Green and G. Hough, Eds.), TAPPI PRESS, Atlanta, (1992), pp. 79-117.
17. Janka, K., Backman, R. and Wallen, J. in *Proceeding of the International Chemical Recovery Conference*, PAPTAC-TAPPI, Whistler, (2001), pp. 79-85.
18. Costa, A.O.S., Martinelli, S.H.S., Biscaia, Jr. E.C., and Lima, E.L. "Descrição empírica da formação de material particulado em uma caldeira de recuperação kraft," *XXX Congresso Brasileiro de Sistemas Particulados–XXX ENEMP*, São Carlos, SP, Brazil, CD-ROM, 2002 (in Portuguese).
19. Neural Networks, Addendum for Version 4, STATISTICA, StatSoft, Inc., Tulsa, (1999).

This paper was originally published in O Papel 65(8): 65(2004), the official publication of the Brazilian Technical Association of Pulp and Paper (ABTCP). It is being reprinted by TAPPI JOURNAL through a cooperative agreement between TAPPI and ABTCP.

This paper is also published on TAPPI's web site <www.tappi.org> and summarized in the April Solutions! for People, Processes and Paper magazine (Vol. 88 No. 4).

INSIGHTS FROM THE AUTHORS

The doctorate degree thesis of Costa presents a hybrid mathematical model to describe the recovery boiler, especially the black liquor burning. For that work, she used different methodologies to model various phenomena that take place in this equipment. In this paper, the authors present the methodology used in Costa's thesis to describe the particulate formation. Costa had found previous research describing the particulate formation in the furnace recovery boiler; however, those studies did not use neural networks.

The most difficult aspect was to obtain industrial data without significant error. This problem was solved adopting a previous treatment of the data set. The major contribution of this study is to present a methodology, based in the industrial data, that describes the particulate formation in a kraft furnace.

We believe that that mills can use this methodology to model the particulate formation in the recovery boiler. The obtained model can be used to predict the operational conditions that promote low particulate formation. The next step in this work is to obtain models to describe other phenomena in pulp and paper mills.

Costa is with Curso de Engenharia Sanitária e Ambiental, Diretoria da Área de Ciências Exatas, UnilesteMG, Av. Tancredo de Almeida Neves, 3500, Coronel Fabriciano, MG, CEP 35170-056, Brazil; de Souza is with the Departamento de Engenharia Química, Escola de Química, CP:68542, CEP 21949-900 Universidade Federal do Rio de Janeiro - UFRJ, Rio de Janeiro, Brazil; Biscaia and Lima are with the programa de Engenharia Química (PEQ), COPPE, Universidade Federal do Rio de Janeiro - UFRJ, Rio de Janeiro, CP:68502, CEP 21945-970, Brazil. Email Costa at andreaosc@unilestemg.br and Lima at enrique@peq.coppe.ufrj.br.

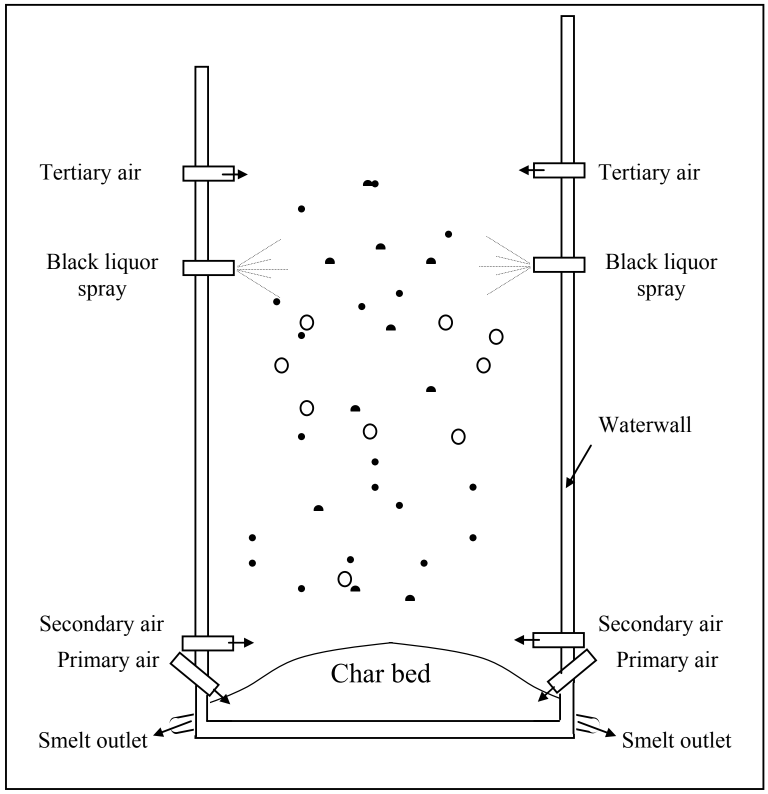

1. Schematic representation of the black liquor burning in a recovery boiler furnace.

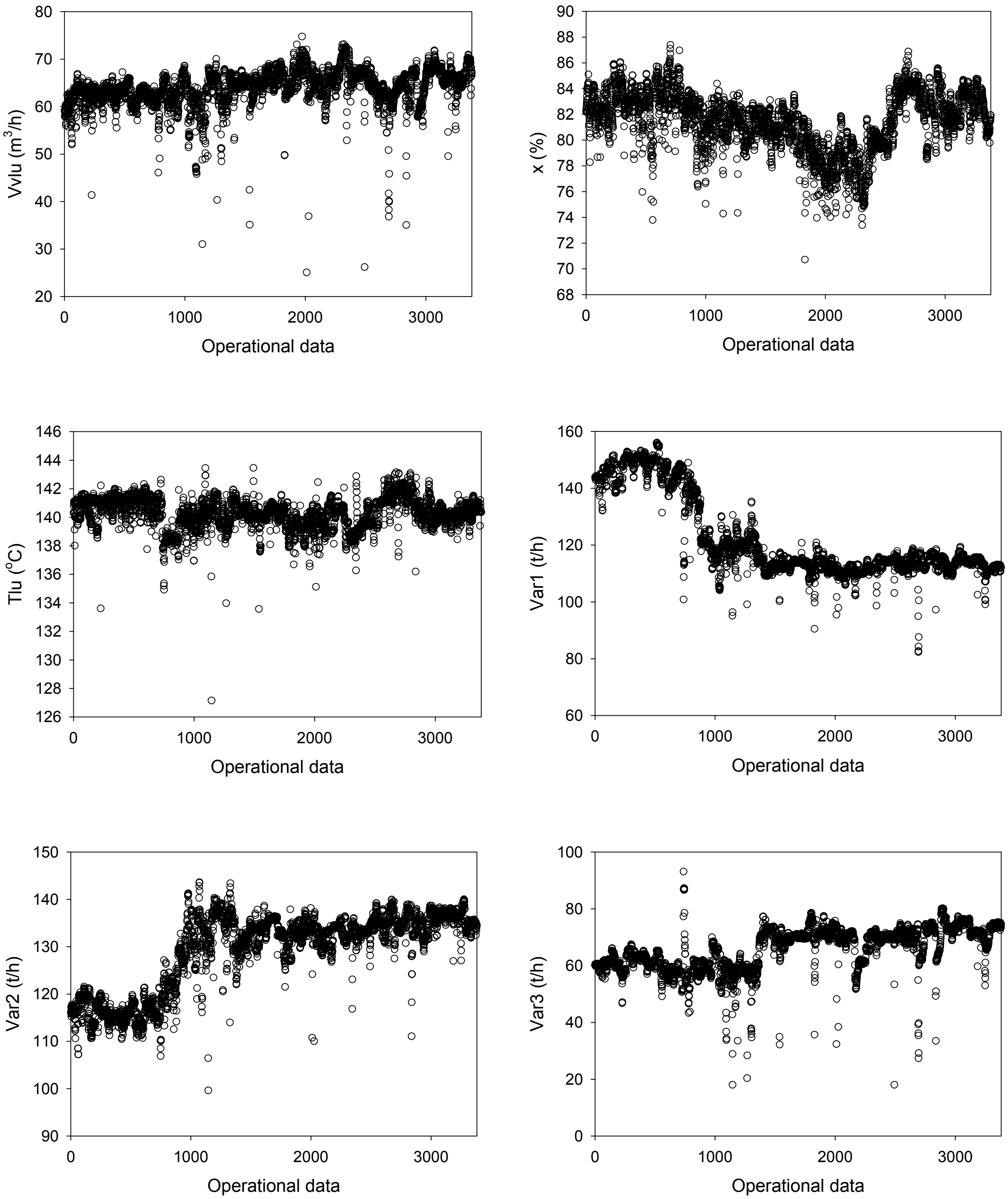

2. Behavior of major operational variables that affect the particulate formation during one year of recovery boiler operation.

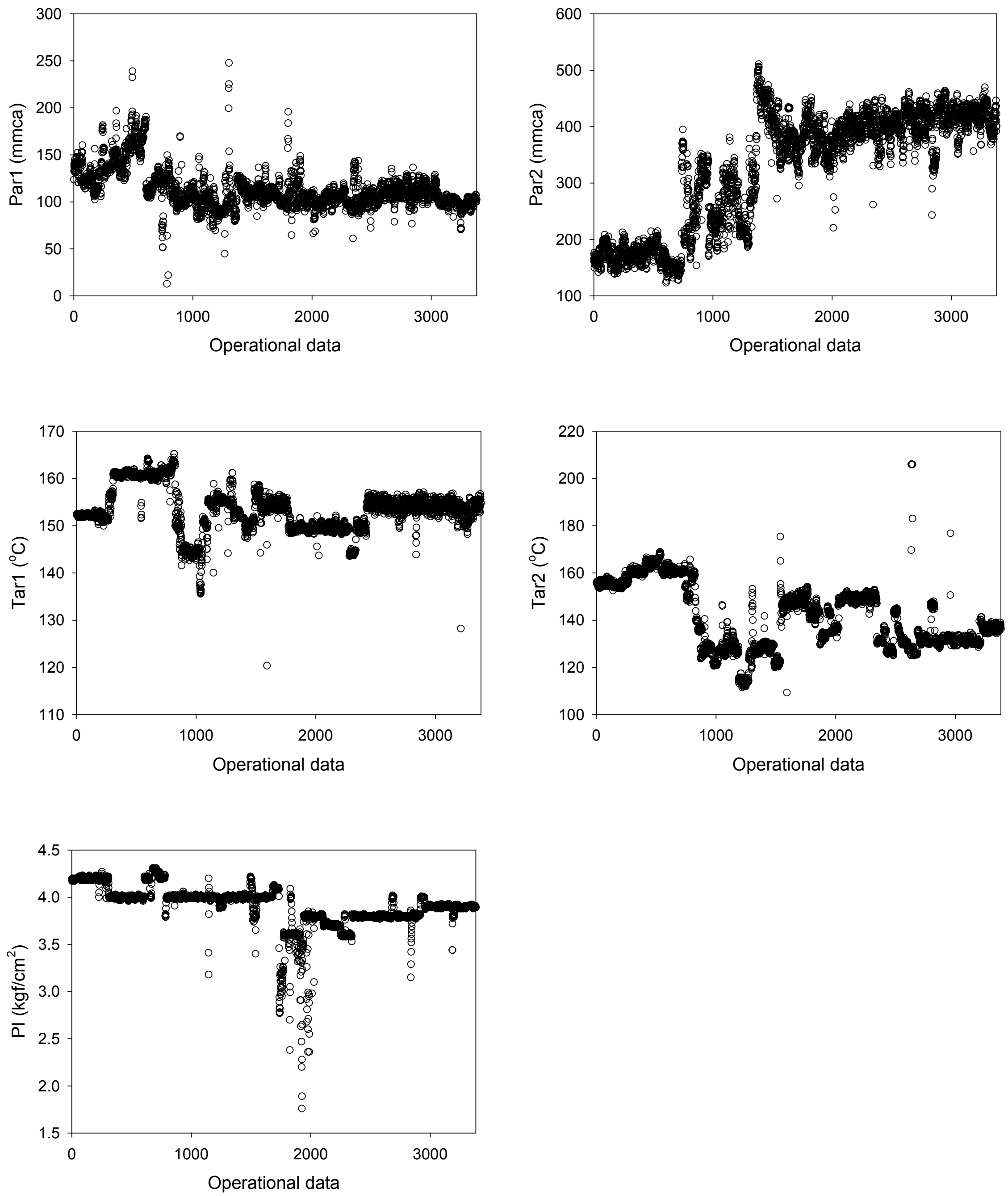

3. Behavior of major operational variables that affect the particulate formation during one year of recovery boiler operation (continuation).

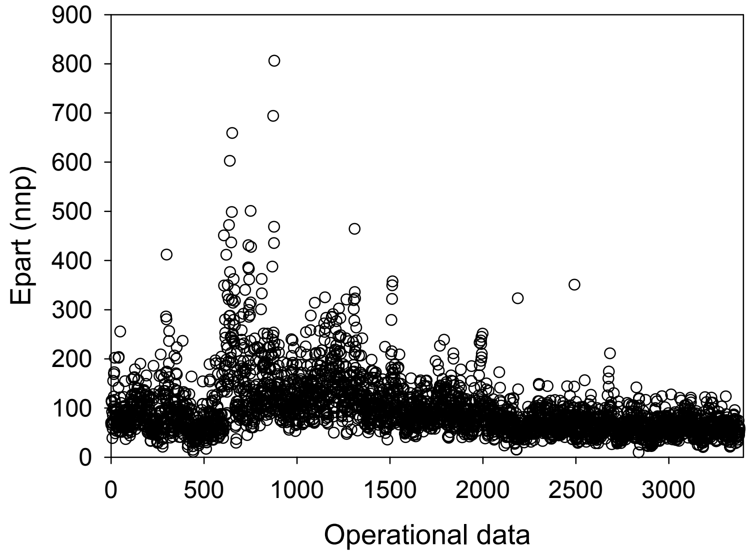

4. Behavior of Epart variable during one year of recovery boiler operation.

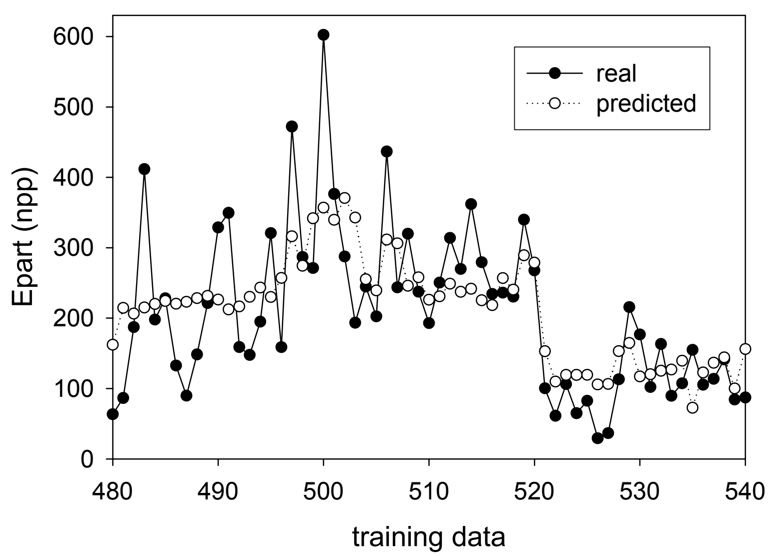

5. Comparison between real (training) and predicted values for the best feedforward neural network.

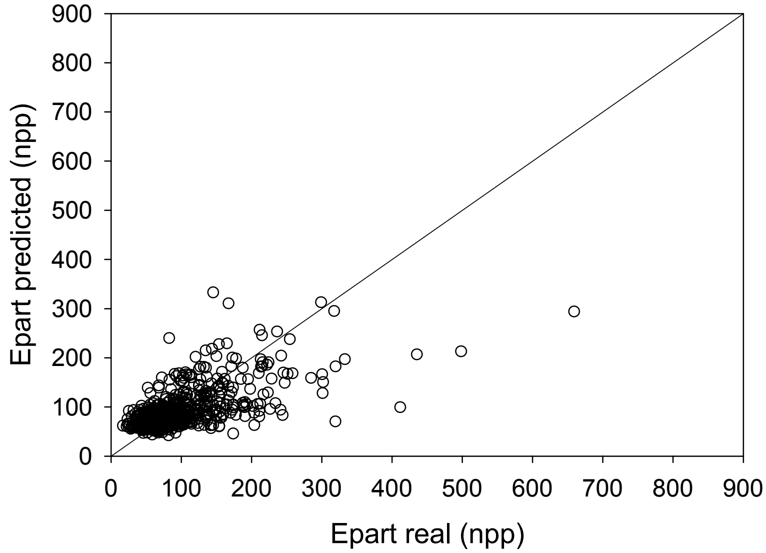

6. Correlation between real (training) and predicted values for the best feedforward neural network.

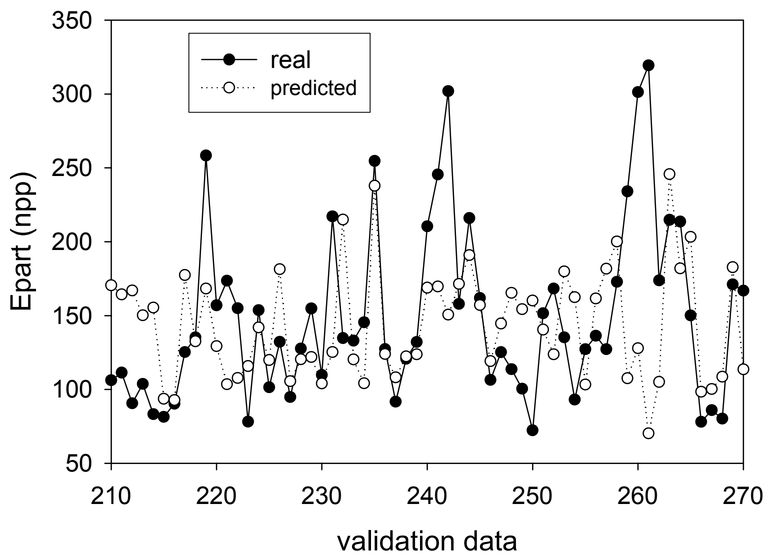

7. Comparison between real (validation) and predicted values for the best feedforward neural network.

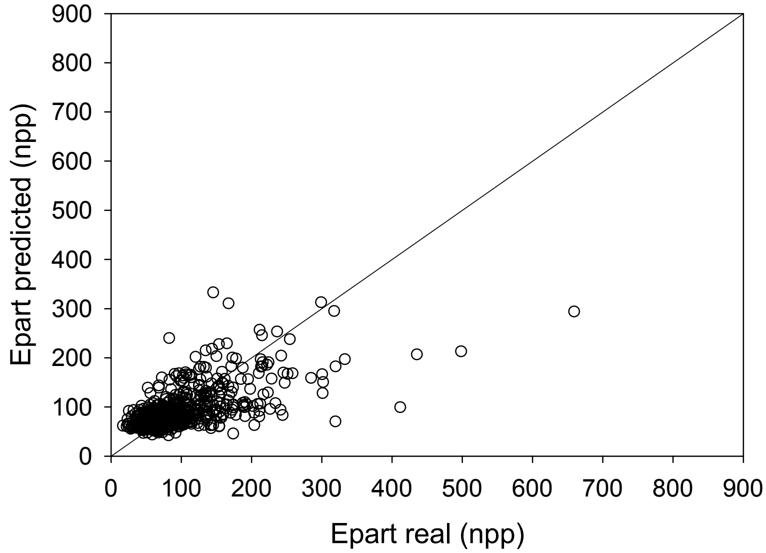

8. Correlation between real (validation) and predicted values for the best feedforward neural network.

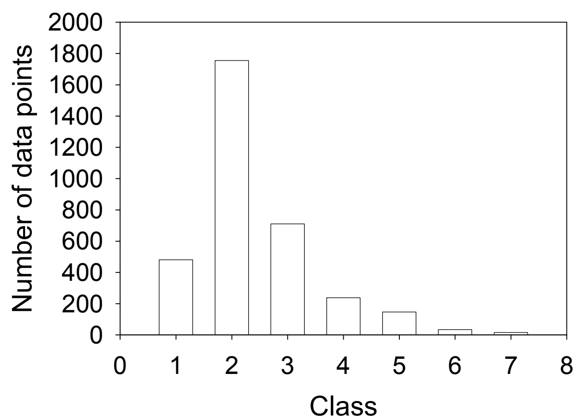

Class	Epart (npp)
1	0 - 50
2	50 - 100
3	100 - 150
4	150 - 200
5	200 - 300
6	300 - 400
7	above 400

9. Distribution of the data considering 7 classes for Epart.

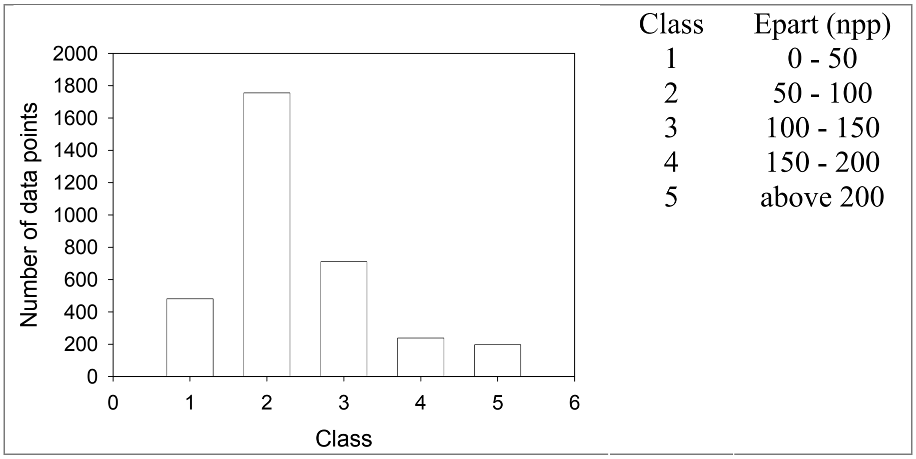

10. Distribution of the data considering 5 classes for Epart.

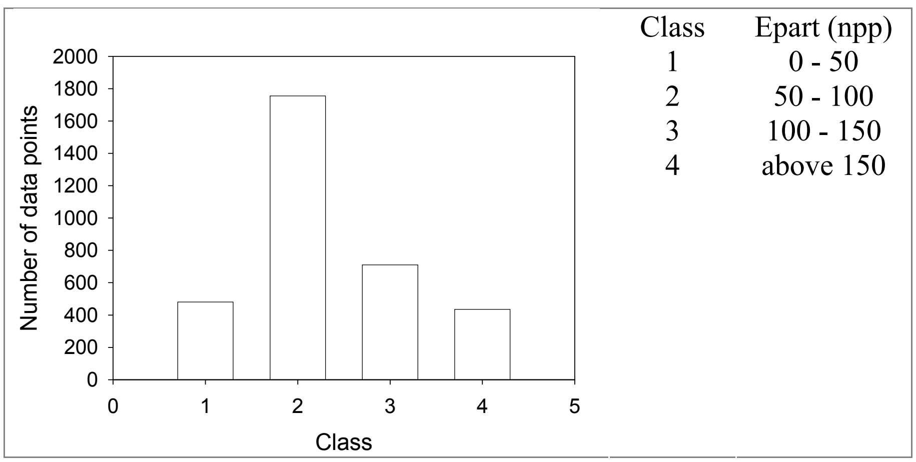

11. Distribution of the data considering 4 classes for Epart.

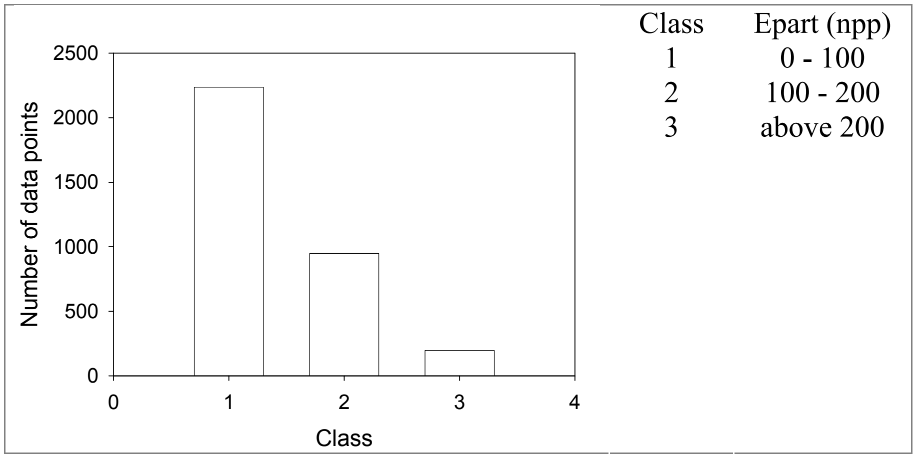

12. Distribution of the data considering 3 classes for Epart.

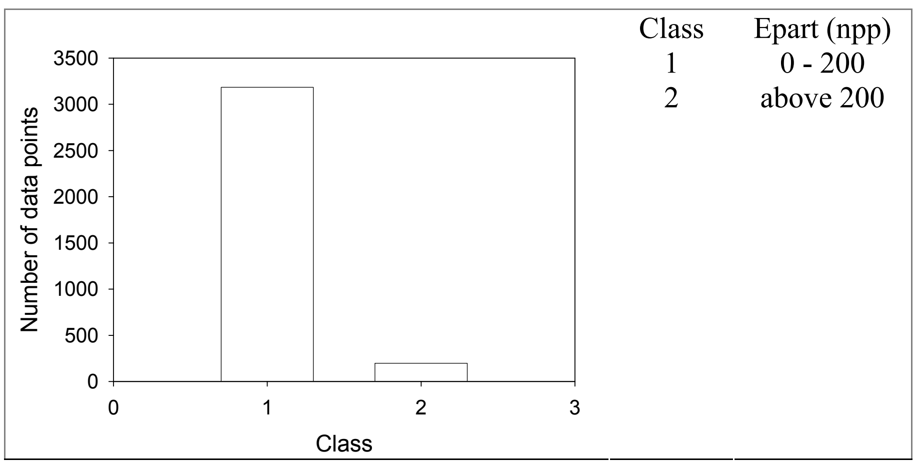

13. Distribution of the data considering 2 classes for Epart.